Bioorganic & Medicinal Chemistry Letters 19 (2009) 4097–4101

Contents lists available at ScienceDirect

Bioorganic & Medicinal Chemistry Letters

journal homepage: www.elsevier.com/locate/bmcl

Aminopiperidine-fused imidazoles as dipeptidyl peptidase-IV inhibitors

Scott D. Edmondson [a,*], Anthony Mastracchio [a], Jason M. Cox [a], George J. Eiermann [b], Huaibing He [c], Kathryn A. Lyons [c], Reshma A. Patel [d], Sangita B. Patel [e], Aleksandr Petrov [b], Giovanna Scapin [e], Joseph K. Wu [d], Shiyao Xu [c], Bing Zhu [c], Nancy A. Thornberry [d], Ranabir Sinha Roy [d], Ann E. Weber [a]

[a] Department of Medicinal Chemistry, Merck & Co. Inc., PO Box 2000, Rahway, NJ 07065, USA
[b] Lead Optimization Pharmacology, Merck & Co. Inc., PO Box 2000, Rahway, NJ 07065, USA
[c] Preclinical Drug Metabolism and Pharmacokinetics, Merck & Co. Inc., PO Box 2000, Rahway, NJ 07065, USA
[d] Department of Metabolic Disorders, Merck & Co. Inc., PO Box 2000, Rahway, NJ 07065, USA
[e] Global Structural Biology, Merck & Co. Inc., PO Box 2000, Rahway, NJ 07065, USA

ARTICLE INFO

Article history:
Received 1 May 2009
Revised 29 May 2009
Accepted 2 June 2009
Available online 6 June 2009

Keywords:
Dipeptidyl peptidase-IV
DPP-4
DPP-IV
Dipeptidyl peptidase 8
DPP-8
DPP-9
Quiescient peptidyl peptidase
QPP
GLP-1
Glucagon-like peptide 1
Benzimidazole
Imidazopyridine
Buchwald coupling
Sitagliptin

ABSTRACT

A new series of DPP-4 inhibitors derived from piperidine-fused benzimidazoles and imidazopyridines is described. Optimization of this class of DPP-4 inhibitors led to the discovery of imidazopyridine **34**. The potency, selectivity, cross-species DMPK profiles, and in vivo efficacy of **34** is reported.

Since the approval of sitagliptin (**1**) by the US Food and Drug Administration in 2006, selective dipeptidyl peptidase IV (DPP-4) inhibitors have established themselves as an important new option for the treatment of type 2 diabetes.[1] In vivo, DPP-4 is responsible for the inactivation of glucagon-like peptide 1 (GLP-1) and glucose-dependent insulinotropic polypeptide (GIP), both of which enhance insulin secretion in a glucose-dependent manner. Additionally, GLP-1 stimulates insulin biosynthesis, inhibits glucagon secretion, slows gastric emptying, reduces appetite, and stimulates the regeneration and differentiation of islet β-cells.[2,3] DPP-4 inhibitors increase circulating GLP-1 and GIP levels in humans, which leads to decreased blood glucose levels, hemoglobin A_{1c} levels, and glucagon levels. DPP-4 inhibitors such as sitagliptin possess advantages over alternative diabetes therapies including a lowered risk of hypoglycemia, a potential for weight loss, and the potential for the regeneration and differentiation of pancreatic β-cells.[3,4]

Aminocyclohexane **2** was identified in an effort to restrict the rotation of sitagliptin (**1**) while maintaining excellent DPP-4 inhibition potency (Fig. 1).[5] The cyclohexane ring can be exchanged with an *N*-aryl aminopiperidine ring to afford a series of DPP-4 inhibitors that possess similar potency to cyclohexylamine analogs.[6] Although many of these aminopiperidines (e.g., **3**) exhibit excellent rat pharmacokinetic profiles, they also possess inferior off-target selectivity profiles. By fusing heterocycles to this piperidine ring to provide imidazole derivatives **4**, we sought to improve the off-target selectivity profile of compounds in this series while maintaining potent DPP-4 inhibition and excellent rat pharmacokinetic profiles.

The synthesis of fused aminopiperidines began by converting lactam **5**[6] to methyl imidate **6** using Meerwein's reagent (Scheme 1). Treatment of **6** with either 2-aminoacetophenone hydrochlo-

* Corresponding author. Tel.: +1 732 594 0287.
E-mail address: scott_edmondson@merck.com (S.D. Edmondson).

0960-894X/$ - see front matter © 2009 Elsevier Ltd. All rights reserved.
doi:10.1016/j.bmcl.2009.06.011

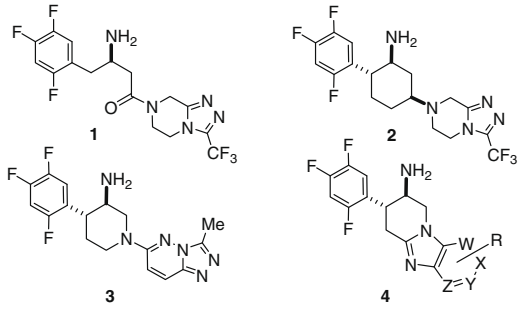

Figure 1. Potent and selective DPP-4 inhibitors, including sitagliptin (**1**), aminocyclohexane **2**, aminopiperidine **3**, and fused imidazole derivatives **4**.

ride or benzoic hydrazide in ethanol afforded the corresponding phenyl linked triazole and imidazole derivatives **7** and **8**, respectively. Hydrolysis of the ethyl ester, Curtius rearrangement, and Cbz deprotection then afforded the final DPP-4 inhibitors **9** and **10**.[7]

Benzimidazole and imidazopyridine derivatives were synthesized as shown in Scheme 2. Protection of the lactam **5** with 4,4′-dimethoxybenzhydrol was followed by ester hydrolysis and Curtius rearrangement to afford the carboxybenzyl (Cbz) protected amine **11**. Next, the Cbz group was exchanged with a Boc group and the secondary lactam was liberated using ceric ammonium nitrate (CAN). Exposure of the free lactam to *ortho* bromo or iodo aro-

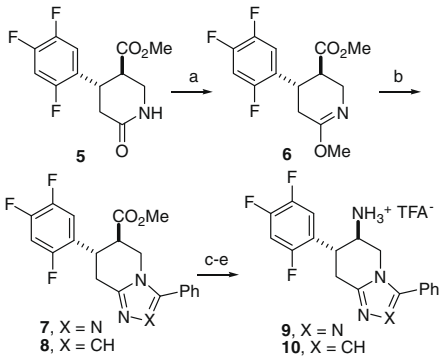

Scheme 1. Synthesis of DPP-4 inhibitors **9** and **10**. Reagents and conditions: (a) Me_3OBF_3, CH_2Cl_2 (76% yield); (b) $PhCOYNH_2$, EtOH, Δ (Y = NH or CH_2); (c) $LiOH_{aq}$, MeOH, THF; (d) DPPA, TEA, tol; BnOH, Δ; (e) H_2, $Pd(OH)_2$, EtOAc, MeOH; then reverse phase purification with 1% TFA in H_2O/CH_3CN.

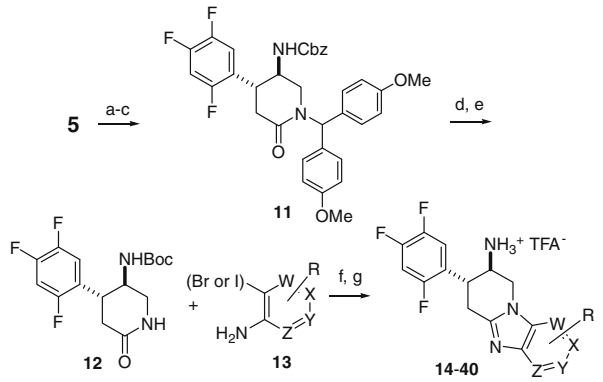

Scheme 2. Synthesis of DPP-4 inhibitors **14**–**40**. Reagents and conditions: (a) $(4\text{-MeOPh})_2CHOH$, H_2SO_4, HOAc (47% yield); (b) $LiOH_{(aq)}$, THF (80% yield); (c) DPPA, TEA, tol; BnOH, Δ; (65% yield); (d) $Pd(OH)_2$, H_2, MeOH, Boc_2O (73% yield); (e) CAN, CH_3CN, H_2O, 0 °C (75% yield of **12**); (f) CuI, $MeNHCH_2CH_2NHMe$, K_2CO_3, toluene, Δ; (g) TFA, CH_2Cl_2 (33–80% yield, two steps).

matic amines (i.e., **13**) under Buchwald's copper-catalyzed coupling conditions[8] then afforded the corresponding benzimidazoles and imidazopyridines in a single reaction. Importantly, this represents a new methodology for the synthesis of benzimidazoles or imidazopyridines. The same transformation could also be accomplished in a three step sequence (not pictured) by first using similar coupling conditions to attach *ortho* bromo-nitrobenzenes to lactam **12**, then reducing the nitro group to an amino group, and finally heating to induce the cyclocondensation that forms the corresponding benzimidazole. The brevity of the single step protocol described in Scheme 2 together with the increased availability of a variety of the starting aminoarenes **13**, however, allowed for a much more efficient method to synthesize analogs. Removal of the Boc group with strong acid then furnished analogs **14**–**40**.[7]

Compounds were tested for inhibition of DPP-4 and selectivity over DPP-4-like activity and/or structural homolog (DASH) proteins including quiescent cell proline peptidase (QPP, DPP-II), prolyl endopeptidase (PEP), aminopeptidase P (APP), prolidase, DPP-8, and DPP-9.[9,10] In general, all compounds possessed excellent selectivity (>1000-fold) over PEP, APP, and prolidase. Fused imidazoles displayed excellent selectivity for DPP-4 inhibition over all counter screens, including DPP-8 and DPP-9.[11] The improved DPP-4 potency of benzimidazole **14** compared to phenyl triazole **9** and phenyl imidazole **10** (Fig. 2) suggested that benzimidazole derivatives warranted further optimization.

In general, the addition of most substituents onto the benzimidazole improved DPP-4 inhibition potency (Table 1). Non-polar substituents (**15**–**24**) generally exhibited moderate improvements in potency over unsubstituted benzimidazole **14**, but many of these analogs exhibited sub-optimal selectivity over QPP (<1000-fold). The 6-fluoro derivative **17** and 5-trifluoromethyl derivative **23** exhibited the most promising profiles, with DPP-4 IC_{50}'s of 17 nM and 14 nM and QPP selectivities of 1400-fold and 2900-fold, respectively.

Introduction of polar substituents onto the 5-position of the benzimidazole ring typically resulted in enhancements in DPP-4 potency and QPP selectivity. Methyl sulfone **25** exhibits excellent DPP-4 potency (DPP-4 IC_{50} = 4.2 nM) and excellent selectivity over QPP, DPP-8 and DPP-9 (IC_{50}'s >100,000). Compared to **25**, the corresponding ethyl sulfone possessed a twofold decrease in DPP-4 intrinsic potency (**26**, DPP-4 IC_{50} = 8.0 nM) and shifting the methyl sulfone to the 6-position resulted in a 13-fold decrease in DPP-4 potency (**27**, DPP-4 IC_{50} = 56 nM). Replacement of the methyl sulfone with a carboxylic acid at the 5-position results in another potent and selective DPP-4 inhibitor (**28**, DPP-4 IC_{50} = 13 nM), but increasing steric bulk to a dimethyl carboxamide afforded a compound with diminished DPP-4 inhibition (**29**, DPP-4 IC_{50} = 52 nM) relative to the carboxylic acid. The placement of polar electron donating substituents onto the 5-position of the benzimidazole ring also afforded potent and selective DPP-4 inhibitors such as a methanesulfonamide **30** and acetamide **31** (DPP-4 IC_{50}'s = 7.1 nM and 8.6 nM, respectively).

The enhanced potency of polar electron donating and polar electron withdrawing substituents at the 5-position of the benz-

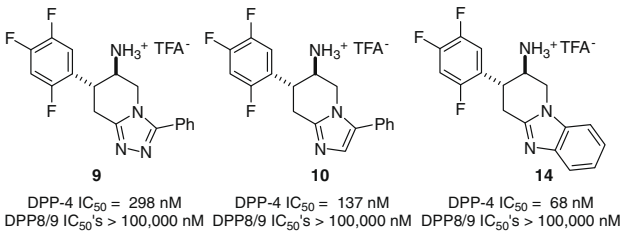

Figure 2. Aminopiperidine-fused heterocycle DPP-4 inhibitors.

Table 1
Piperidine fused benzimidazoles derived DPP-4 inhibitors

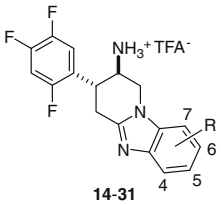

14-31

Compd	R=	IC_{50} (μM)			
		DPP-4	QPP	DPP-8	DPP-9
14	H	0.068	22	>100	>100
15	4-F	0.030	5.5	>100	>100
16	5-F	0.077	16	>100	71
17	6-F	0.017	23	>100	79
18	4,6-DiF	0.047	2.3	>100	60
19	4,5,6-TriF	0.022	6.5	>100	60
20	5-MeO	0.028	73	>100	73
21	6-CF_3O	0.053	22	45	>100
22	5-Me	0.018	33	>100	>100
23	5-CF_3	0.014	41	>100	>100
24	6-CF_3	0.047	8.3	>100	81
25	5-SO_2Me	0.0042	88	>100	>100
26	5-SO_2Et	0.0080	>100	>100	>100
27	6-SO_2Me	0.056	>100	>100	>100
28	5-CO_2H	0.013	>100	>100	>100
29	5-$CONMe_2$	0.052	98	>100	>100
30	5-$NHSO_2$Me	0.0071	74	>100	63
31	5-NHCOMe	0.0086	54	53	>100

imidazole ring suggests that both the position and nature of the substituent might interact with the DPP-4 binding pocket. To better understand the important binding interactions of these benzimidazoles, methyl sulfone **25** was co-crystallized with DPP-4 and an X-ray crystal structure of the ligand-enzyme complex was obtained. An overlay of sitagliptin (**1**, yellow) and methyl sulfone **25** (purple) with DPP-4 shows that the major interactions of these inhibitors with DPP-4 are similar (Fig. 3).[12] The carbonyl group in sitagliptin (**1**) and one of the benzimidazole nitrogen atoms in **25** are each positioned to interact with a water molecule at the same location in the DPP-4 binding pocket. Similarly, the triazole of **1** and one of the oxygens from the sulfone moiety of **25** are each positioned to interact with a second water molecule in the DPP-4 binding pocket.

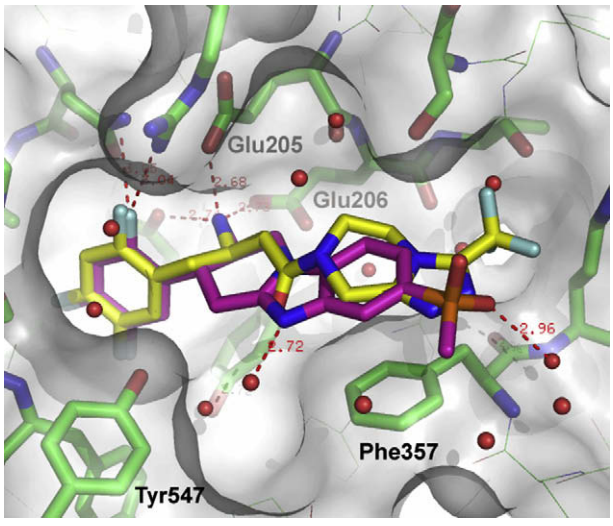

Figure 3. X-ray crystal structures of methylsulfone **25** (purple) and sitagliptin **1** (yellow) bound to DPP-4.[12] Interactions of **1** and **25** with DPP-4 are shown in red dotted lines.

Furthermore, the benzimidazole ring itself appears to stack efficiently with Phe357, similar to the triazole ring in sitagliptin.

Analysis of the X-ray crystal structure of **25** and the SAR from Table 1 suggest that small polar groups on the 5-position of the benzimidazole ring enhance DPP-4 potency and improve selectivity over other DASH proteins. To further develop the SAR in this class of DPP-4 inhibitors, a series of imidazopyridines were next evaluated (Table 2).

Imidazopyridines **34a** and **35** (DPP-4 IC_{50}'s = 6.7 nM and 12 nM, respectively) each exhibited superior DPP-4 inhibition potencies compared to **32** and **33** (DPP-4 IC_{50}'s = 329 nM and 51 nM, respectively). Installation of substituents adjacent to the pyridine in **34a** afforded inhibitors with excellent potency at DPP-4 but typically with reduced selectivity over QPP, DPP-8 and/or DPP-9 (e.g., **35**, **36**, and **38**) relative to **34a**. As expected, a Tris–HCl salt **34b** possesses similar DPP-4 potency and off-target selectivity compared to the corresponding trifluoroacetic acid salt **34a**.

Inhibitors that possessed superior potency and selectivity profiles were evaluated in rat pharmacokinetic studies (Table 3). Activity at hERG was also routinely measured in order to assess potential cardiovascular liabilities.[13] Selectivity over hERG was sub-optimal (⩽1000-fold) for benzimidazoles **17**, **23**, and **30** and the rat oral bioavailabilities of **17** and **28** were only moderate (F_{rat} = 37% and 24%, respectively). Methyl sulfone **25** exhibited the best overall profile in the benzimidazole series with respect to selectivity over hERG (~9000-fold) and rat pharmacokinetic profile (F_{rat} = 68%, $t_{1/2}$ = 3.4 h). Imidazopyridines **34a**, **35**, **38**, and **39** all possessed excellent selectivities over hERG (⩾5000-fold) and excellent overall rat pharmacokinetic profiles (F_{rat} ⩾ 87%, $t_{1/2}$ ⩾ 2.6 h).

DPP-4 inhibition data in Tables 1 and 2 reflect binding of inhibitors to the recombinant human enzyme in buffer (i.e., intrinsic potency). In order to more accurately predict in vivo potency, inhibitors **25**, **34**, **35**, **38**, and **39** were evaluated further in an assay using endogenous human DPP-4 in the presence of 50% human

Table 2
Piperidine fused imidazopyridines as DPP-4 inhibitors

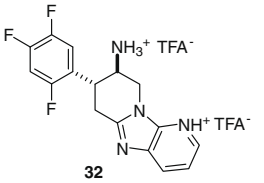

32

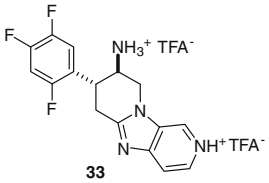

33

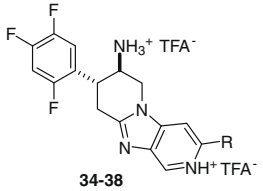

34-38

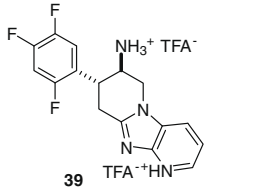

39

Compd	R=	IC_{50} (μM)			
		DPP-4	QPP	DPP-8	DPP-9
32	—	0.329	23	>100	>100
33	—	0.051	>100	72	8.4
34a[a]	H	0.0067	>100	>100	>100
34b[a]	H	0.0083	>100	>100	>100
35	F	0.012	19	>100	65
36	Cl	0.015	4.6	42	36
37	Me	0.023	49	24	47
38	CF_3	0.011	13	31	91
39	—	0.015	19	>100	>100

[a] Compound **34a** is a *bis*-TFA salt and **34b** is a *Tris*–HCl salt.

Table 3
Pharmacokinetic properties of selected DPP-4 inhibitors (1/2 mg/kg iv/po) and hERG binding

Compd	Species	Clp (mL/min/kg)	$t_{1/2}$ (h)	F (%)	hERG IC_{50} (μM)
17	Rat	25	1.4	37	17
23	Rat	4.8	7.6	55	7.5
25	Rat	2.2	3.4	63	38
28	Rat	61	0.4	24	—
30	—	—	—	—	2.5
34a	Rat	8.7	2.6	140	89
34b	Mouse	36	1.9	73	—
	Dog	2.7	13	120	—
	Rhesus	35	1.0	11	—
35	Rat	0.5	17	87	81
38	Rat	1.4	8.7	110	57
39	Rat	3.9	3.8	96	90

serum (i.e., serum shifted potency, Table 4).[14] Methyl sulfone **25** and imidazopyridine **34** are the most potent DPP-4 inhibitors in the presence of human serum, and imidazopyridines **35** and **39** show similar serum shifted potencies as **34**. On the other hand, trifluoromethyl substituted imidazopyridine **38** exhibits a 2–3-fold reduction in DPP-4 inhibition potency in the presence of serum relative to **25** and **34**.

Aminopiperidine DPP-4 inhibitors such as **3** possess sub-optimal off-target activities at the L-type calcium channel and CYP2D6.[6] To further differentiate **25**, **34**, **35**, and **39** from this previous class of DPP-4 inhibitors and from each other, each analog was evaluated for binding to the rabbit L-type calcium channe1[15] and inhibition of CYP2D6[16] (Table 4). Analogs **25**, **34**, and **39** all possess >1000-fold selectivity (vs intrinsic DPP-4 potency) over binding to the L-type calcium channel, but fluoropyridine **35** is only 125-fold selective over this ion channel. Imidazopyridine **34** showed the best selectivity over CYP2D6 inhibition (>1000-fold vs intrinsic DPP-4 potency), while **25** and **39** exhibit inferior selectivities of only 360-fold and 350-fold, respectively. Additional in vitro profiling of **34** in an extensive panel of over 150 receptor and ion channel binding and enzyme inhibition assays showed no significant activity at 10 μM (data not shown).

Based on the superior profile of imidazopyridine **34** with respect to in vitro DPP-4 potency, off-target selectivity, and rat pharmacokinetics, this compound was selected for further in vivo and DMPK profiling. Hydrochloride salt **34b** possesses good oral bioavailability in mice (F = 73%), a moderate clearance (Clp = 35 mL/min/kg) and a half-life of 1.9 h. In dogs, **34b** exhibited an excellent overall PK profile (F = 120%, Clp = 2.7 mL/min/kg, $t_{1/2}$ = 13 h). In monkeys, however, **34b** displayed a relatively poor overall PK profile (F = 11%, Clp = 35 mL/min/kg, $t_{1/2}$ = 1.0 h).

To better understand the observed species differences in PK profiles, **34** was incubated with liver microsomes to assess its propensity to undergo oxidative metabolism. Compound **34** showed similar stability across four species with 83%, 92%, 69% and 97% parent remaining after 60 min incubations in rat, dog, rhesus, and human liver microsomes, respectively. Incubation of **34** with hepatocytes (1 μM concentration), however, demonstrated a definitive decrease in stability in rhesus hepatocytes relative to other species. Only 35% parent remained after 60 min in rhesus hepatocytes while 94%, ~99%, and ~99% parent was recovered at 60 min following rat, dog, and human hepatocyte incubations, respectively. The hepatocyte results suggest that the human PK profile of **34** will more closely resemble the rat and dog PK profiles than rhesus.

Next, **34b** was assessed for its ability to improve glucose tolerance in lean mice (murine DPP-4 IC_{50} = 45 nM for **34b**).[14] Administration of single oral doses reduced the blood glucose excursion in an oral glucose tolerance test (OGTT) in a dose-dependent manner from 0.1 mg/kg (27% reduction) to 3.0 mg/kg (49% reduction) when administered 60 min before an oral dextrose challenge (5 g/kg). The PD profile of compound **34** was also assessed in a separate OGTT study in lean mice. Plasma DPP-4 inhibition, compound concentration, and active GLP-1 levels were measured 10 min after a dextrose challenge. Maximal efficacy was achieved at 1 mg/kg, corresponding to 88% DPP-4 inhibition and 691 nM plasma levels. At the maximally efficacious dose (1 mg/kg), a 2–3-fold increase of active GLP-1 levels was observed, which is analogous to active GLP-1 levels increases reported after a glucose challenge in DPP-4 deficient mice.[17] Based on the relative potency of **34b** at human DPP-4 compared to mouse DPP-4 and the reduced non-covalent plasma protein binding of **34b** in human relative to mouse plasma (55% vs 41% free fraction, respectively), the corresponding level of DPP-4 inhibition in humans can be estimated at 97 nM plasma levels. This correlates well with an empirically derived human DPP-4 EC_{80} = 112 nM.[14]

An X-ray crystal structure of imidazopyrazine **34** co-crystallized with DPP-4 (Fig. 4) demonstrates the binding interactions of **34** with the enzyme. An overlay of sitagliptin (**1**, yellow) and **34** (purple) with DPP-4 shows that the major interactions of **34** with DPP-4 are similar to those of methyl sulfone **25**. In the case of **34**, however, the pyridine nitrogen instead of the sulfone oxygen in **25** interacts with a water molecule in the binding pocket.

In conclusion, a new series of DPP-4 inhibitors derived from piperidine-fused benzimidazoles and imidazopyridines are presented which exhibit excellent potency and selectivity profiles. Novel synthetic methodology was described that introduced a one step synthesis of benzimidazoles and imidazopyridines from a δ-lactam and an *ortho* bromo or iodo aromatic amine. Optimization

Table 4
Intrinsic DPP-4 potency (rec hum DPP-4), serum shifted DPP-4 potency (hum DPP-4+50% HS), calcium (Ca) channel, and CYP2D6 activities of selected DPP-4 inhibitors

Compd	IC_{50} (μM)			
	Rec hum DPP-4	Hum DPP-4 +50% HS	Ca	CYP2D6
25	0.0042	0.011	>100	1.5
34a	0.0067	0.016	>100	13
34b	0.0083	0.017	>100	13
35	0.012	0.023	1.5	12
38	0.011	0.032	96	11
39	0.015	0.024	>100	5.2

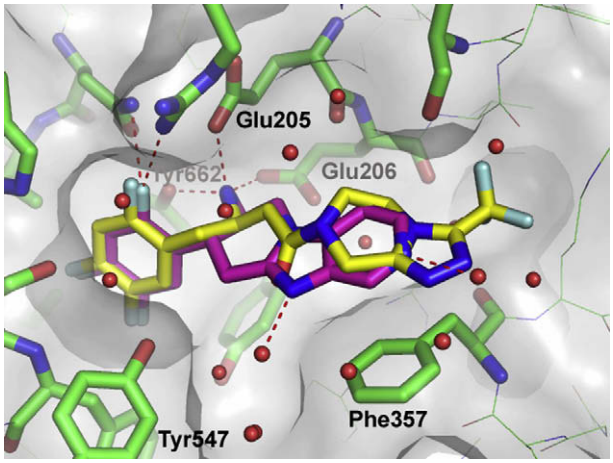

Figure 4. X-ray crystal structures of imidazopyridine **34** (purple) and sitagliptin **1** (yellow) bound to DPP-4.[12] Interactions of **1** and **34** with DPP-4 are shown in red dotted lines.

of this series afforded imidazopyridine **34**, a potent DPP-4 inhibitor with a moderate serum shift that demonstrates an excellent in vitro selectivity and in vivo efficacy profile. Furthermore, compound **34** exhibits a promising preclinical pharmacokinetic profile in rats and dogs. Poor stability of **34** in rhesus monkey hepatocyte incubations suggest that the sub-optimal pharmacokinetic profile in rhesus may not translate to humans. Additional in vitro and in vivo profiling of **34** will be reported in due course.

Acknowledgments

The authors thank I. Capodanno, M. Ferguson, L. de Reus, J. Hausmann, V. Jenning, T. Johnson, J. Mane, C. Nunes, X. Sheng, K. Vakerich, Z. Yao, and B. Wang for dosing the animals used in pharmacokinetic experiments and Y. Yan and T. Biftu for help preparing this manuscript.

Use of the IMCA-CAT beamline 17-ID at the Advanced Photon Source was supported by the companies of the Industrial Macromolecular Crystallography Association through a contract with the Center for Advanced Radiation Sources at the University of Chicago. Use of the Advanced Photon Source was supported by the U.S. Department of Energy, Office of Science, Office of Basic Energy Sciences, under Contract No. W-31-109-Eng-38. Use of beamline X25 of the National Synchrotron Light Source was supported by the Offices of Biological and Environmental Research and of Basic Energy Sciences of the US Department of Energy, and by the National Center for Research Resources of the National Institutes of Health.

References and notes

1. (a) Karasik, A.; Aschner, P.; Katzeff, H.; Davies, M. J.; Stein, P. P. *Curr. Med. Res. Opin.* **2008**, *24*, 489; (b) Thornberry, N. A.; Weber, A. E. *Curr. Top. Med. Chem.* **2007**, *7*, 557–568; (c) Edmondson, S. D.; Kim, D. Selective Dipeptidyl Peptidase IV Inhibitors for the Treatment of Type 2 Diabetes: The Discovery of JANUVIA™ (Sitagliptin). In *Methods and Principles in Medicinal Chemistry*; Antitargets Vaz, R. J., Klabunde, T., Eds.; Wiley-VCH, 2008; Vol. 38, pp 401–422.
2. For lead DPP-4 references, see: (a) Havale, S. H.; Pal, M. *Bioorg. Med. Chem.* **2009**, *17*, 1783; (b) Pei, Z. *Curr. Opin. Drug Disc. Dev.* **2008**, *11*, 512; (c) Ahren, B. *Exp. Opin. Emerg. Drugs* **2008**, *13*, 593; (d) Idris, I.; Donnelly, R. *Diab. Obes. Metab.* **2007**, *9*, 153.
3. For lead GLP-1 references, see (a) Holst, J. J.; Vilsboll, T.; Deacon, C. F. *Mol. Cell. Endocrinol.* **2009**, *297*, 127; (b) Kim, W.; Egan, J. M. *Pharm. Rev.* **2008**, *60*, 470; (c) Holst, J. J. *Physiol. Rev.* **2007**, *87*, 1409.
4. During, M. J.; Cao, L.; Zuzga, D. S.; Francis, J. S.; Fitzsimons, H. L.; Jiao, X.; Bland, R. J.; Klugmann, M.; Banks, W. A.; Drucker, D. J.; Haile, C. N. *Nat. Med.* **2003**, *9*, 1173.
5. (a) Biftu, T.; Scapin, G.; Singh, S.; Feng, D.; Becker, J. W.; Eiermann, G.; He, H.; Lyons, K.; Patel, S.; Petrov, A.; Sinha-Roy, R.; Zhang, B.; Wu, J.; Zhang, X.; Doss, G. A.; Thornberry, N. A.; Weber, A. E. *Bioorg. Med. Chem. Lett.* **2007**, *17*, 3384; (b) Gao, Y.-D.; Feng, D.; Sheridan, R. P.; Scapin, G.; Patel, S. B.; Wu, J. K.; Shang, J.; Sinha-Roy, R.; Thornberry, N. A.; Weber, A. E.; Biftu, T. *Bioorg. Med. Chem. Lett.* **2007**, *17*, 3877.
6. Cox, J. M.; Harper, B.; Mastracchio, A.; Leiting, B.; Sinha Roy, R.; Patel, R. A.; Wu, J. K.; Lyons, K. A.; He, H.; Xu, S.; Zhu, B.; Thornberry, N. A.; Weber, A. E.; Edmondson, S. D. *Bioorg. Med. Chem. Lett.* **2007**, *17*, 4579.
7. (a) Final compounds were characterized by ^{1}H NMR and LC–MS. Detailed procedures and spectral data for selected compounds are described in the following patents: Cox, J. M.; Edmondson, S. D.; Mastracchio, A. Fused Aminopiperidines as Dipeptidyl Peptidase-IV Inhibitors for the Treatment or Prevention of Diabetes WO 2006/058064, filed Nov. 22, 2005.; (b) Cox, J. M.; Edmondson, S. D.; Mastracchio, A. Fused Aminopiperidines as Dipeptidyl Peptidase-IV Inhibitors for the Treatment or Prevention of Diabetes WO 2007/024993, filed Aug. 22, 2006; Biftu, T.; Cox, J. M.; Edmondson, S. D.; Mastracchio, A. Fused Aminopiperidines as Dipeptidyl Peptidase-IV Inhibitors for the Treatment or Prevention of Diabetes WO 2007/070434, filed Dec. 8, 2006.
8. Klapars, A.; Huang, X.; Buchwald, S. L. *J. Am. Chem. Soc.* **2002**, *124*, 7421.
9. IC_{50} determinations for DPP-4 and QPP were carried out as described in Leiting, B.; Pryor, K. D.; Wu, J. K.; Marsilio, F.; Patel, R. A.; Craik, C. S.; Ellman, J. A.; Cummings, R. T.; Thornberry, N. A. *Biochem. J.* **2003**, *371*, 525.
10. All DPP-4 IC_{50}'s are an average of $n \geqslant 4$, with standard deviations less than 60% of the average.
11. For a discussion of the relevance of selectivity over DPP-8 and DPP-9, see Lankas, G. R.; Leiting, B.; Sinha Roy, R.; Eiermann, G. J.; Beconi, M. G.; Biftu, T.; Chan, C.-C.; Edmondson, S.; Feeney, W. P.; He, H.; Ippolito, D. E.; Kim, D.; Lyons, K. A.; Ok, H. O.; Patel, R. A.; Petrov, A. N.; Pryor, K. A.; Qian, X.; Reigle, L.; Woods, A.; Wu, J. K.; Zaller, D.; Zhang, X.; Zhu, L.; Weber, A. E.; Thornberry, N. A. *Diabetes* **2005**, *54*, 2988.
12. The atomic coordinates for the X-ray structures of DPP-4 in complex with **25** and **34** have been deposited into the RCSB protein data bank under RCSB ID codes RCSB052890 and RCSB052891, and under PDB ID codes 3HAB and 3HAC, respectively.
13. IC_{50} determinations for hERG was carried out as described in Friesen, R. W.; Ducharme, Y.; Ball, R. G.; Blouin, M.; Boulet, L.; Cote, B.; Frenette, R.; Girard, M.; Guay, D.; Huang, Z.; Jones, T. R.; Laliberte, F.; Lynch, J. J.; Mancini, J.; Martins, E.; Masson, P.; Muise, E.; Pon, D. J.; Siegel, P. K. S.; Styhler, A.; Tsou, N. N.; Turner, M. J.; Young, R. N.; Girard, Y. *J. Med. Chem.* **2003**, *46*, 2017.
14. Edmondson, S. D.; Mastracchio, A.; Mathvink, R. J.; He, J.; Harper, B.; Park, J.-J.; Beconi, M.; Di Salvo, J.; Eiermann, G. J.; He, H.; Leiting, B.; Leone, J. F.; Levorse, D. A.; Lyons, K.; Patel, R. A.; Patel, S. B.; Petrov, A.; Scapin, G.; Shang, J.; Sinha Roy, R.; Smith, A.; Wu, J. K.; Xu, S.; Zhu, B.; Thornberry, N. A.; Weber, A. E. *J. Med. Chem.* **2006**, *49*, 3614.
15. IC_{50} determinations for rabbit calcium channel were carried out as described in Shoemaker, H.; Hicks, P.; Langer, S. *J. Cardiovasc. Pharm.* **1987**, *9*, 173.
16. Rendic, S. *Drug. Metab. Rev.* **2002**, *34*, 83.
17. Marquet, D.; Baggio, L.; Kobayashi, T.; Bernard, A.-M.; Pierres, M.; Nielsen, M.; Ribel, U.; Watanabe, T.; Drucker, D. J.; Wagtmann, N. P. *Proc. Natl. Acad. Sci. U.S.A.* **2000**, *97*, 6874.